

# 11

## Thermoelectric Module Design Theories

---

11.1	Introduction .....	11-1
11.2	Power Output and Conversion Efficiency .....	11-2
11.3	Design Considerations and Optimization .....	11-4
11.4	Coefficient of Performance and Heat Pumping Capacity .....	11-4
11.5	Fabrication Quality Factor .....	11-7
11.6	Micro/Nano Converters .....	11-8
11.7	Ring-Structure Module .....	11-11
11.8	Summary .....	11-14

Gao Min  
*Cardiff University*

### 11.1 Introduction

---

The basic unit of a thermoelectric (TE) generator or refrigerator is a “thermocouple” shown schematically in [Figure 11.1a](#). It consists of an n-type and a p-type thermoelement connected electrically in series by a conducting strip (usually copper). Although this basic unit can also be employed as the “engineering” building-block for construction of thermoelectric conversion systems, a less complicated approach for system engineers is to employ “thermoelectric module” as the building-block. Figure 11.1b shows schematically a thermoelectric module, which consists of a number of the basic units connected electrically in series but thermally in parallel and sandwiched between two ceramic plates. Thermoelectric modules can be prefabricated as general purpose products in various dimensions. A theoretical model is required in order to evaluate their thermoelectric performances.

The generating performance of a thermoelectric module is gauged primarily by the conversion efficiency and power-per-unit-area, while the cooling performance by the coefficient of performance (COP) and heat-pumping capacity. These quantities may be estimated using a theory developed by Ioffe based on a simplified model in which the thermal and electrical contact resistances had been neglected.<sup>1</sup> Although this theory has proven to be adequate for analysis of large-dimension thermoelectric modules, it becomes inaccurate and sometimes invalid for the modules which possess short thermoelement length. Over the past few years, an improved theory has been developed based on a more realistic model which takes into account the thermal and electrical contact resistances of the modules.<sup>2–10</sup> The improved theory provides a better accuracy for modeling of thermoelectric modules and proves to be very useful in analysis and optimal design of small-dimension thermoelectric modules.

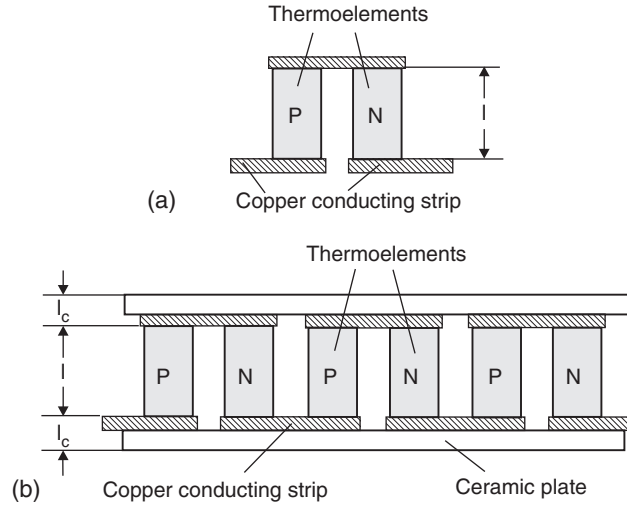


FIGURE 11.1 Basic configuration of a thermoelectric module: (a) basic unit; (b) more realistic model.

## 11.2 Power Output and Conversion Efficiency

Thermoelectric modules convert heat into electricity when operating in the Seebeck mode. The electrical power generated from a module depends upon the numbers of thermocouples in a module, thermoelement configuration, thermoelectric properties of thermoelement materials, thermal, and electrical properties of contact layers, and the temperature difference across the module. Based on a typical module configuration of Figure 11.1b, and taking into account the thermal and electrical contact resistances, it can be shown<sup>6</sup> that when the module operates with a matched load, the output voltage  $V$  and current  $I$  are given by:

$$V = \frac{N\alpha(T_h - T_c)}{1 + 2rl_c/l} \quad (11.1)$$

$$I = \frac{A\alpha(T_h - T_c)}{2\rho(n + l)(1 + 2rl_c/l)} \quad (11.2)$$

where  $N$  is the number of thermocouples in a module,  $\alpha$  the Seebeck coefficient of the thermoelement material employed, and  $\rho$  the electrical resistivity,  $T_h$  and  $T_c$  are temperatures at the hot- and cold-sides of the module, respectively,  $A$  and  $l$  are the cross-sectional area and thermoelement length, respectively,  $l_c$  is the thickness of the contact layer,  $n = 2\rho_c/\rho$  and  $r = \lambda/\lambda_c$  (where  $\rho_c$  is the electrical contact resistivity,  $\lambda_c$  the thermal contact conductivity, and  $\lambda$  the thermal conductivity of thermoelement materials).  $n$  and  $r$  are usually referred to as electrical and thermal contact parameters, respectively. These can be estimated using a method described in Ref. [9]. For commercially available Peltier modules, appropriate values are  $n \sim 0.1$  mm and  $r \sim 0.2$ .

Figure 11.2 shows the current-per-unit-area of a thermoelement,  $I/A$ , and the voltage-per-thermocouple,  $V/N$ , as a function of thermoelement length for different temperature differences. The voltage increases with an increase in thermoelement length, while the current exhibits a maximum at a shorter-length regime. For a given temperature difference and thermoelement length, the ratios  $I/A$  and  $V/N$  of a module fabricated using currently available materials and technologies can be estimated from Figure 11.2. If the cross-sectional area of the thermoelements and the number of thermocouples in a module are known, the electrical current and voltage delivered to a matched load can be determined.

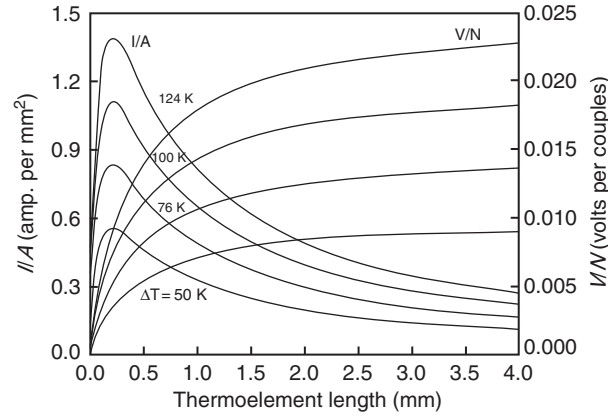


FIGURE 11.2  $V/N$  and  $I/A$  vs. thermoelement length for different temperature differences.

The power output  $P$  and conversion efficiency  $\phi$  of a thermoelectric module, when operated with a matched load, can be expressed as<sup>3,4</sup>

$$P = \frac{\alpha^2}{2\rho} \frac{AN(T_h - T_c)^2}{(n + l)(1 + 2rl_c/l)^2} \quad (11.3)$$

$$\phi = \frac{\left( \frac{T_h - T_c}{T_h} \right)}{\left( 1 + 2r \frac{l_c}{l} \right)^2 \left[ 2 - \frac{1}{2} \left( \frac{T_h - T_c}{T_h} \right) + \left( \frac{4}{ZT_h} \right) \left( \frac{l + n}{l + 2rl_c} \right) \right]} \quad (11.4)$$

where  $Z = \alpha^2/(\rho\lambda)$  is the thermoelectric figure-of-merit of the materials. Figure 11.3 shows the power-per-unit-area  $p(=P/AN)$  and conversion efficiency vs. the thermoelement length for different temperatures. It can be seen that in order to obtain high conversion efficiency, the module should be designed with long thermoelements. However, if a large power-per-unit-area is required, the thermoelement length should be optimized at a relatively shorter length. It is apparent that the

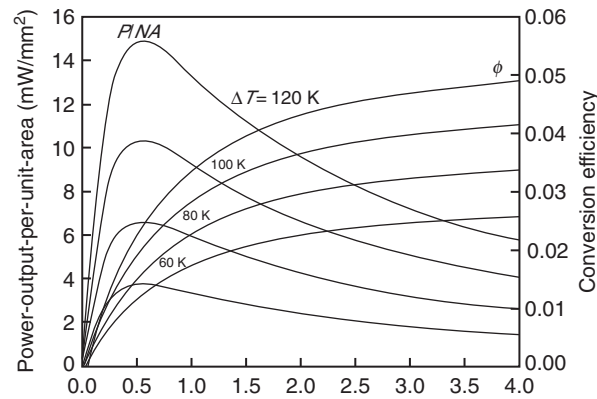


FIGURE 11.3 Power-per-unit-area and conversion efficiency vs. thermoelement length for different temperature differences.

optimum design of a thermoelectric module is likely to be a compromise between obtaining high conversion efficiency or large power output.

### 11.3 Design Considerations and Optimization

The parameters appearing in Equation 11.1 through Equation 11.4 can be grouped into three categories:

1. *Specifications*: The operating temperatures  $T_c$  and  $T_h$ , the required output voltage  $V$ , current  $I$ , and power output  $P$ .
2. *Material parameters*: The thermoelectric properties  $\alpha$ ,  $\sigma$ ,  $\lambda$  and the module contact properties  $n$  and  $r$ .
3. *Design parameters*: The thermoelement length  $l$ , the cross-sectional area  $A$ , and the number of the thermocouples  $N$ .

The specifications are usually provided by customers depending on the requirements of a particular application. The material parameters are restricted by currently available materials and module fabricating technologies. Consequently, the main objective of thermoelectric module design is to determine a set of design parameters which meet the required specifications at minimum cost. The number of the thermocouples,  $N$ , required in a module can be determined using Equation 11.1, while the cross-sectional area,  $A$ , can be obtained from Equation 11.2. The determination of  $N$  and  $A$  for a given thermoelement length is usually a straightforward calculation. However, the determination of thermoelement length involves a rather complicated optimization procedure driven by its economic viability.

In general, a high conversion efficiency is required if the heat source (fuel) is expensive, while a large power-per-unit-area is required if fabrication cost is to be reduced. In practice, the cost-per-kilowatt-hour (£/kWh) is generally used as a yardstick of the economic viability of a generator. Using the improved theory Equation 11.3 and Equation 11.4, the cost per-kilowatt-hour,  $c$ , of electricity generated using a thermoelectric module may be estimated using<sup>6</sup>

$$c = \frac{c_m}{p\Delta t} + \frac{c_f}{\phi} \quad (11.5)$$

where  $c_m$  is the fabrication cost of a thermoelectric module,  $c_f$  the input thermal energy cost per kilowatt hour (e.g., £/kWh),  $\Delta t$  the operation period, and  $p$  and  $\phi$  are the power-output and conversion efficiency, respectively, of a thermoelectric module. Figure 11.4 shows the cost-per-kilowatt-hour vs. the conversion efficiency and power-per-unit-area for different fuel costs for  $\Delta T = 100$  K. It can be seen that a trade-off between the conversion efficiency and power output is dependent on the cost of heat source employed. If the heat source employed is expensive, the module should be designed to obtain large conversion efficiency. However, if the heat source is inexpensive or essentially free, such as in the case of waste heat, increasing the power-per-unit-area will result in a reduction in the cost of electricity generation (£/kWh). This can be achieved by employing thermoelements with shorter length.

### 11.4 Coefficient of Performance and Heat Pumping Capacity

Thermoelectric modules can be used for refrigeration when operated in the Peltier mode. Similarly, based on Figure 11.1b and taking into account thermal and electrical contact resistances, the COP,  $\eta$ , and heat pumping capacity per unit area,  $q$ , of a thermoelectric cooling module are given by<sup>8</sup>

$$\eta = \frac{l}{l + 2rl_c} \left( \frac{T_c}{T_h - T_c} \frac{\left(1 + \frac{Z\bar{T}l}{n+l}\right)^{1/2} - \frac{T_h}{T_c}}{\left(1 + \frac{Z\bar{T}l}{n+l}\right)^{1/2} + 1} - \frac{rl_c}{l} \right) \quad (11.6)$$

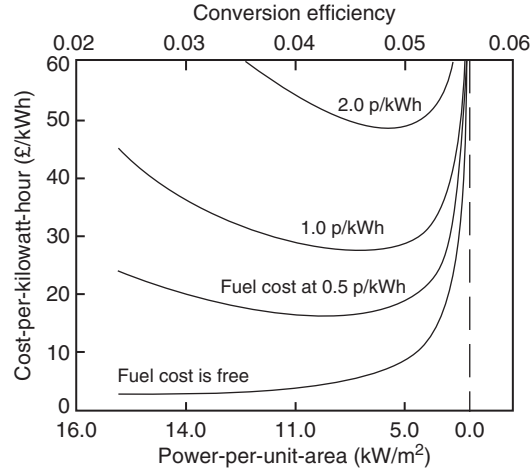


**FIGURE 11.4** The cost-per-kilowatt-hour as a function of conversion efficiency and power-per-unit-area for  $\Delta T = 100$  K.

$$q = \frac{\lambda(\Delta T_{\max} - \Delta T)}{l + 2rl_c + rl_c/\eta} \quad (11.7)$$

where  $\bar{T} = (T_h + T_c)/2$  is the mean temperature across the thermoelectric module and  $\Delta T_{\max} = ZT_c^2/2$  is the maximum temperature difference when the load at the cold-side is zero.

Figure 11.5 shows the COP of a realistic thermoelectric module as a function of thermoelement length for  $\Delta T = 25$  K with  $T_h$  at 300 K (a typical condition for domestic refrigeration). It can be seen that the COP increases with an increase in thermoelement length. The effect of contact resistances on the COP becomes significant when the thermoelement length is relatively short. For commercially available modules the values are,  $n \approx 0.1$  mm,  $r \approx 0.2$ ,  $l_c = 0.7$  mm, and  $z = 2.8 \times 10^{-3} \text{ K}^{-1}$ .<sup>9</sup> It can be seen that a sharp decrease in COP occurs when the thermoelement length of commercially available modules is below 1.5 mm. Evidently, designers should be aware that it is essential to reduce the contact resistances if short thermoelement length is employed.

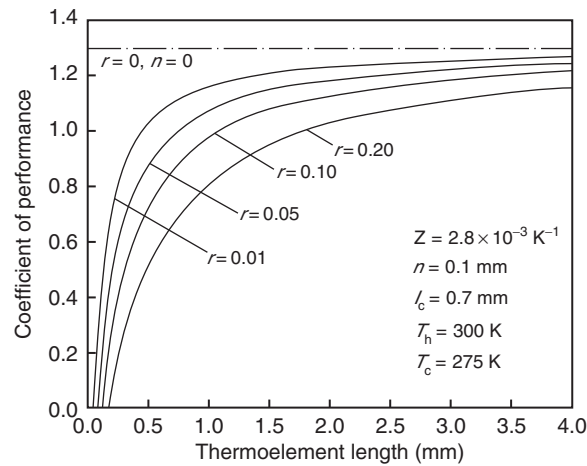


**FIGURE 11.5** The COP as a function of thermoelement length for different  $r$ .

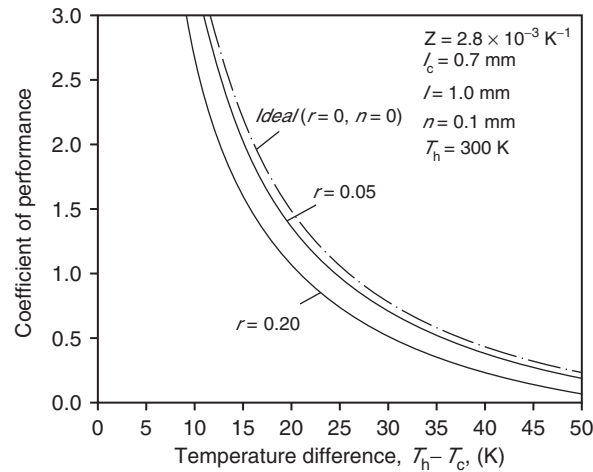


**FIGURE 11.6** The COP as a function of the temperature difference across the module for different contact parameters.

Figure 11.6 shows the COP as a function of temperature difference for a module with thermoelement length of 1.0 mm. The COP decreases with an increase in temperature difference. A temperature difference of at least 25 to 30 K is usually necessary to achieve satisfactory cooling performance for a typical domestic refrigerator. This corresponds to a COP of around 0.5 to 0.7 for a thermoelectric refrigerator, which is about half that of a commercial compressor-type refrigerator. For given thermoelectric materials, the COP of modules may further be improved up to 60% by reducing contact resistances and ceramic thickness.

Figure 11.7 shows the heat pumping capacity per unit area vs. thermoelement length. The heat pumping capacity increases with decreasing thermoelement length until it reaches a maximum and then decreases with a further reduction in the thermoelement length. Improving the contact resistances make little difference to modules with a long thermoelement ( $l > 1.5 \text{ mm}$ ). However, the improvement of the heat pumping capacity due to reducing the contact resistances is significant for modules with short

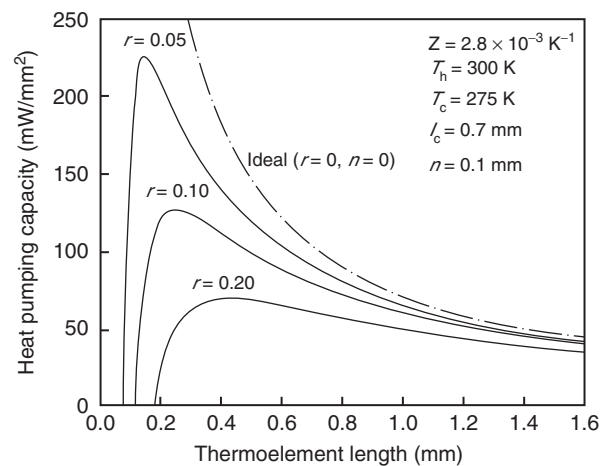


**FIGURE 11.7** The heat pumping capacity as a function of thermoelement length for different contact parameters.

thermoelements. For modules with a thermoelement length of 0.3 mm, the heat pumping capacity can be doubled by reducing the thermal contact parameter  $r$  from currently 0.2 to 0.1.

## 11.5 Fabrication Quality Factor

An important consequence of the improved theory is to show that the generating or cooling performances of a thermoelectric module are also affected by its contact parameters  $n$ ,  $r$ , and contact layer thickness  $l_c$ . Appropriate selection of contact materials and formation of electrical and thermal junctions are also important factors in the design and fabrication of thermoelectric modules. Rewriting Equation 11.3:

$$P = FN\Delta T^2 \left( \frac{\alpha^2}{2\rho} \right) \left( \frac{A}{l} \right) \quad (11.8)$$

where

$$F = \frac{1}{\left( 1 + \frac{n}{l} \right) \left( 1 + \frac{2rl_c}{l} \right)^2} \quad (11.9)$$

$F$  is referred to as the *fabrication quality factor*. In ideal case,  $F$  approaches unity when contact properties  $n$  and  $r$  approach zero. However, in practice, contact resistances always exist, resulting in  $F < 1$ . Evidently, a key objective in module fabrication is to develop suitable fabrication technologies and procedures that minimize contact resistances. It can also be seen that once the contact properties  $n$  and  $r$  are given,  $F$  will be affected by thermoelement length and contact layer thickness. Figure 11.8 shows  $F$  as a function of thermoelement length,  $l$ . The curves are calculated values of the factor  $F$  using Equation 11.9 based on  $n = 0.1$  mm and  $l_c = 1.0$  mm for different  $r$ . A large  $F$  can be obtained by employing very long thermoelements, but at the expense of small power output or heat pumping capacity (as shown in Figure 11.3 and Figure 11.7). Clearly, an ultimate goal in module design and fabrication is to obtain a large  $F$  at a small  $l$ , so that large conversion efficiency and large power output can be achieved in the case of power generation (or large COP and heat pumping capacity in the case of refrigeration).

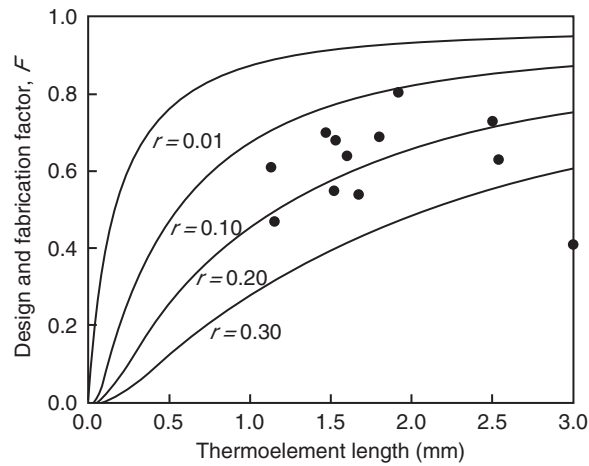


**FIGURE 11.8** The factor  $F$  as a function of thermoelement length for different  $r$  (with  $n = 0.1$  mm and  $l_c = 1$  mm). The curves are calculated from theory and the solid circles are obtained from experiments.

Rewriting Equation 11.8, the design and fabrication quality factor can be expressed as

$$F = \frac{P}{N\Delta T^2 \left( \frac{\alpha^2}{2\rho} \right) \left( \frac{A}{l} \right)} \quad (11.10)$$

Equation 11.10 provides a useful procedure to determine the factor  $F$  from experiments. The  $F$  values of several commercially available thermoelectric modules have been estimated experimentally as shown by the solid circles in Figure 11.8.  $F$  value is about 0.6 to 0.8 for a thermoelement length of around 1.5 mm. This indicates that adequate thermoelectric performances can be obtained from conventional modules which usually possess thermoelement length longer than 1 mm. However,  $F$  will decrease considerably with a decrease in thermoelement length. This will result in poor performances in micro/nano thermoelectric converters, if any. It is apparent that substantial improvement in contact resistances (thermal and electrical) is necessary for micro/nano scales applications. The use of the  $F$  factor provides quantitative analysis of module fabrication technology requirements on contact parameters.

## 11.6 Micro/Nano Converters

The development of thermoelectric micro/nano converters, particularly those compatible with standard silicon IC technology, is anticipated to provide many promising applications in microelectronics, microsystems, and nanotechnology. Currently, two possible configurations have been proposed for fabricating thermoelectric microconverters using MEMS technology.<sup>11–13</sup> Figure 11.9a and b show a vertical and horizontal structure, respectively. In the vertical structure, a thermoelectric microconverter is fabricated with its thermoelement length aligned in the same direction as the thin film growth

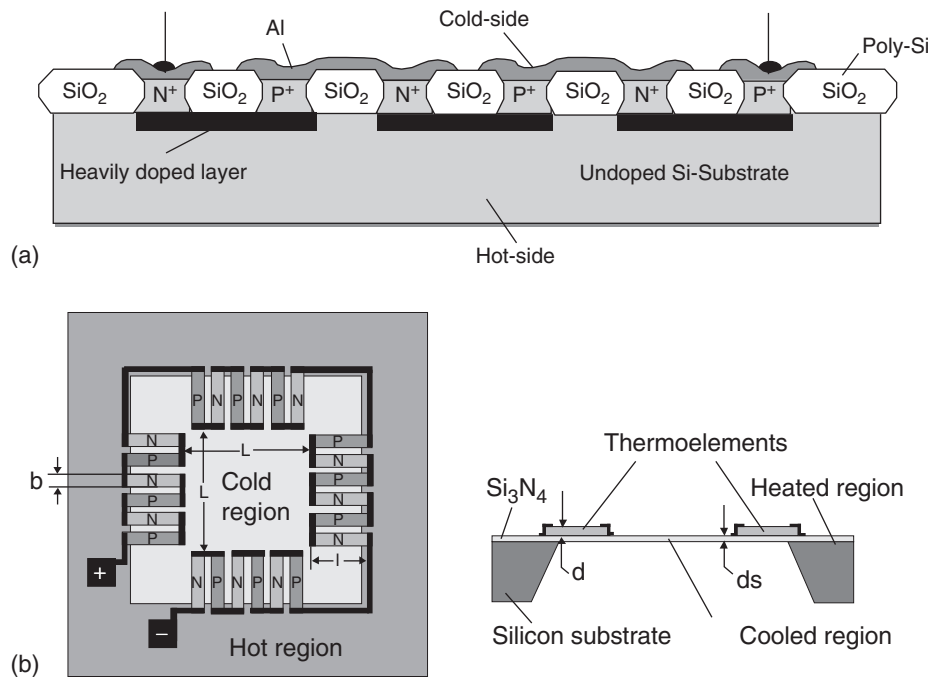


FIGURE 11.9 Schematic thermoelectric microconverters: (a) vertical structure; (b) horizontal structure.



direction, so that the temperature gradient is applied or generated perpendicular to the substrate surface. In the horizontal structure, thermoelements are “lying” on the substrate surface and the temperature gradient is applied or generated along the substrate surface.

The design theory described above can be applied directly to the vertical structure without need for modification. However, the length of the thermoelements in this case is likely to be very short (a few to tens of micrometers). As shown in Figure 11.8, very small contact parameters  $n$  and  $r$  are essential to obtain an adequate  $F$  factor. Clearly, successful realization of a vertically structured microconverter depends on substantial improvement in the electrical and thermal contact properties.

Relatively long thermoelement can be fabricated using the horizontal structure. This helps to ease the difficulty in obtaining very small contact parameters required in the vertical structure. However, a thermal bypass is introduced due to substrate underneath the thermoelements in the horizontal structure. A modified theory has been developed which takes into account the influence of the substrate thermal bypass and radiation loss due to large surface areas of thermoelement.<sup>14</sup> In the case when a microconverter is employed for cooling applications, the maximum temperature difference is given by<sup>14</sup>

$$\Delta T_{\max} \cong \frac{(\alpha^2/\rho\lambda)T_c^2}{(1 + n/l)[1 + (\lambda_s d_s/\lambda d) + (Ll(h + 4\epsilon\sigma T_h^3)/4\lambda d)]} \quad (11.11)$$

where  $h$  is the convection heat transfer coefficient;  $\epsilon$  the emissivity of the central to-be-cooled region;  $\sigma$  the Stefan–Boltzmann constant;  $\lambda_s$  the thermal conductivity of the substrate;  $L$  the length of the central to-be-cooled region;  $d$  and  $d_s$  are the thicknesses of thermoelements and substrate, respectively. The COP can be expressed as

$$\eta = \left( \frac{l^2}{l^2 + 2rd} \right) \left[ \frac{T_c}{T_h - T_c} \frac{(1 + Z_s T_m)^{1/2} - T_h/T_c}{(1 + Z_s T_m)^{1/2} + 1} - \frac{rd}{l^2} \right] \quad (11.12)$$

where

$$Z_s = \frac{Z}{\left[ 1 + \frac{\lambda_s d_s}{\lambda d} + \frac{Ll(h + 4\epsilon\sigma T_h^3)}{4\lambda d} \right]} \quad (11.13)$$

and  $Z$  is the thermoelectric figure-of-merit of the thin-film materials. The heat pumping capacity is given by

$$Q_c = \frac{4dLl\lambda(\Delta T_{\max} - \Delta T)}{l^2 + 2rd + rd/\eta} \quad (11.14)$$

Figure 11.10 displays  $\Delta T_{\max}$  against thermoelement thickness  $d$  for different membrane thickness  $d_s$ . The results were calculated by assuming that  $Z = 2.8 \times 10^{-3} \text{ K}^{-1}$  for n-type and p-type thermoelectric materials,  $\lambda = 1.5 \text{ W/mK}$ ,  $\lambda_s = 2 \text{ W/mK}$ ,  $d = 2 \text{ }\mu\text{m}$ ,  $d_s = 1 \text{ }\mu\text{m}$ ,  $L = 1 \text{ mm}$ ,  $T_h = 300 \text{ K}$ ,  $4\epsilon\sigma T_h^3 = 6.12 \text{ W/m}^2\text{K}$ , and  $h \approx 0$  (operating in vacuum). It can be seen that the membrane thickness significantly affects the maximum temperature difference of a thermoelectric microcooler. In order to obtain adequate cooling performance, the membrane thickness has to be of the same order of magnitude as that of thermoelements, or preferably smaller. A  $\Delta T_{\max}$  of about 30 K can be obtained if the thickness for the thermoelement and membrane is around 1  $\mu\text{m}$ . However,  $\Delta T_{\max}$  reduces to less than 10 K when the membrane thickness increases to around 10  $\mu\text{m}$ . Figure 11.11 shows the COP as a function of cold-side temperature for different substrate thickness. The adverse effect of thermal bypass is evident. It can be seen that when operating over a temperature difference of 25 K with thermoelement and substrate thicknesses around 2  $\mu\text{m}$ , the COP is only about 40% that of a free-standing device. However, improvement in COP can be

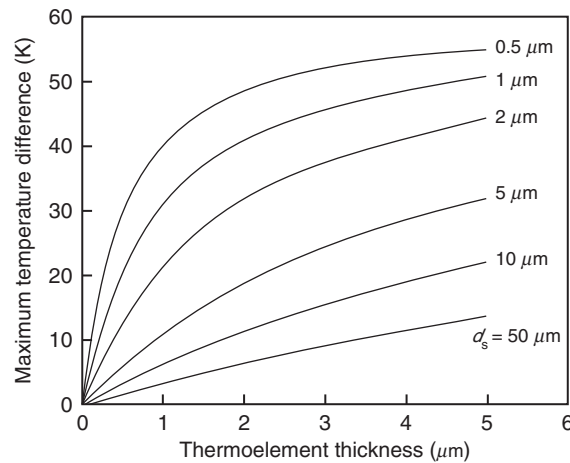


**FIGURE 11.10** Calculated maximum temperature difference of a thermoelectric microconverter as a function of thermoelement thickness for different substrate thicknesses.

achieved by increasing thermoelement thickness and/or decreasing substrate thickness. Figure 11.12 displays the heat pumping capacity as a function of cold-side temperature for different substrate thickness. The effect of substrate thickness is also evident.

Figure 11.13 shows the  $\Delta T_{\max}$  as a function of thermoelement length. Curve *a* is calculated based on currently available contact parameters  $n \approx 0.1$  mm and  $r \approx 0.2^9$  with a substrate thickness of  $1 \mu\text{m}$ . It represents a realistically achievable cooling performance of a “horizontal” thermoelectric microcooler. In order to obtain a temperature difference of 30 K, a thermoelement length of  $100 \mu\text{m}$  is required. However, it is anticipated that the electrical and thermal contact resistances of thin-film devices are usually lower than in their bulk counterparts because of a better control of interface properties. Assuming  $n \approx 0.05$  mm and  $r \approx 0.05$  for thin-film devices, the  $\Delta T_{\max}$  of corresponding microconverter is indicated by curve *b*. In this case, a shorter length of  $50 \mu\text{m}$  can be employed to obtain the same 30 K cooling effect. Curve *c* shows the upper bound of a thermoelectric microcooler which has a  $1 \mu\text{m}$  thick

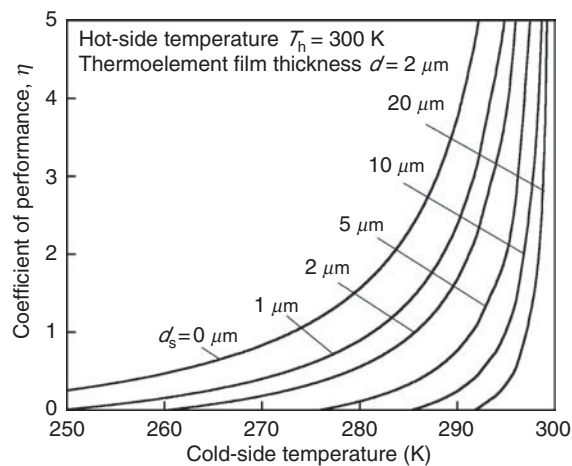


**FIGURE 11.11** Calculated COP of a thermoelectric microconverter as a function of cold-side temperature for different substrate thicknesses.

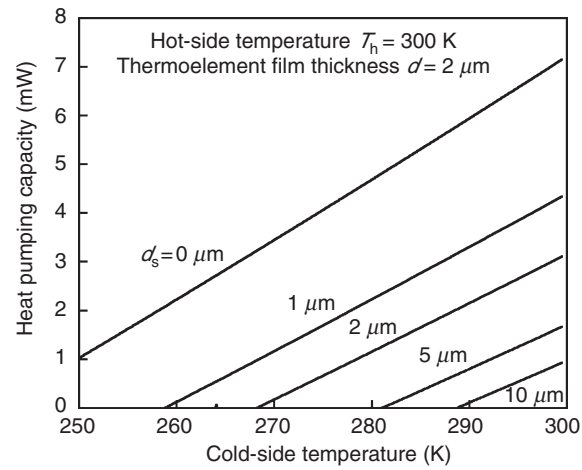


**FIGURE 11.12** Calculated heat pumping capacity of a thermoelectric microconverter as a function of cold-side temperature for different substrate thicknesses.

substrate, while curve *d* shows the possible  $\Delta T_{\max}$  without substrate. It is evident that very small  $n$ ,  $r$ , and  $d_s$  are crucial to successful fabrication of horizontal structure thermoelectric microconverters.

## 11.7 Ring-Structure Module

Conventional thermoelectric converters usually possess a plate-like structure as shown in Figure 11.1. This configuration is usually suitable for applications when heat flows in parallel directions. For applications where heat flows in radial direction, a ring-structured configuration is more advantageous. Figure 11.14a shows the schematic of a ring-structure thermoelectric converter proposed recently.<sup>15</sup> It consists of a coaxial assembly of a number of flat annular “washers” which are made of n-type and p-type thermoelectric materials and connected alternately in series. These are joined alternately at their inner and outer peripheries by copper rings in the manner of compressed concertina bellows. The gaps between n-type and p-type washers underneath or above copper rings are filled with electrically and

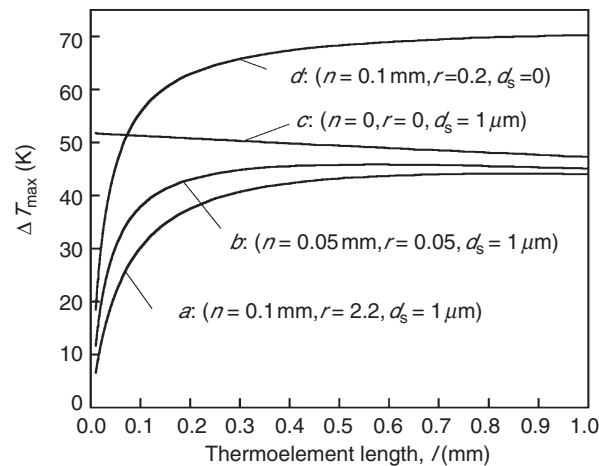


**FIGURE 11.13** Calculated maximum temperature difference as a function of thermoelement length.

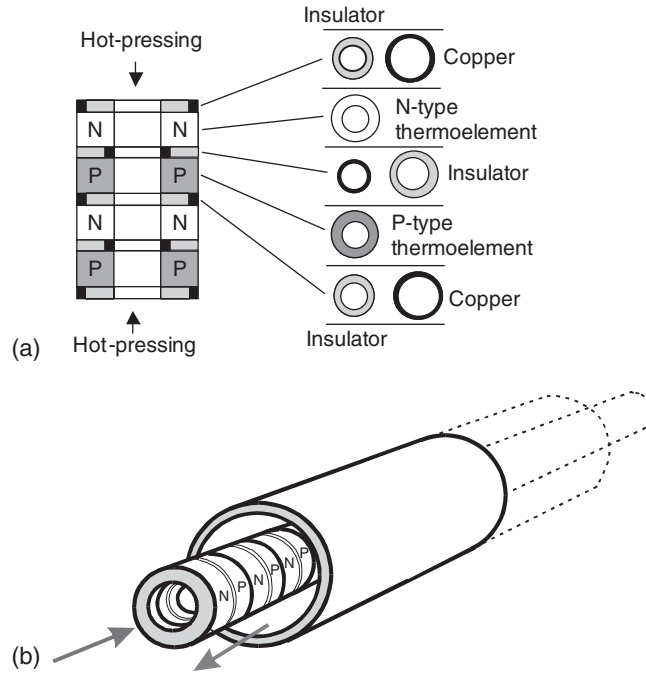


FIGURE 11.14 Schematic of a ring-structure thermoelectric converter: (a) basic structure; (b) thermoelectric tube.

thermally insulating materials. Figure 11.14b shows the schematic of a thermoelectric “tube,” constructed based on the above mentioned fabrication procedure. When hot water flows through the tube, a temperature difference will be established between the inner and outer surfaces of the tube. With the inner tube surface being one thermocouple junction and outer tube surface the other, electrical power will be generated. Clearly, an important advantage of this novel configuration is that the thermoelectric converter itself is as a conductor and a generator as well.

Based on a single thermocouple of ring-structured configuration and assuming that n-type and p-type thermoelements exhibit very similar thermoelectric properties, i.e.,  $|\alpha_n| = |\alpha_p| = \alpha$ ,  $\rho_n = \rho_p = \rho$  and  $\lambda_n = \lambda_p = \lambda$ . Neglecting the contact resistance of interface layers, the electrical resistance of a ring-structure thermocouple can be expressed as

$$R = 2 \int_{r_o}^{r_i} \frac{\rho(r)}{2\pi tr} dr = \frac{(\rho_n + \rho_p)}{\pi t} \ln\left(\frac{r_i}{r_o}\right) = \frac{2\rho}{\pi t} \ln\left(\frac{r_i}{r_o}\right) \quad (11.15)$$

where  $r_o$  and  $r_i$  are the inside and outside diameters, respectively, and  $t$  is the thickness of the ring. The corresponding thermal conductance is given by

$$K = \frac{2\pi t(\lambda_n + \lambda_p)}{\ln(r_i/r_o)} = \frac{4\pi t\lambda}{\ln(r_i/r_o)} \quad (11.16)$$

In general, the Seebeck coefficient is independent of thermoelement geometry. It can be shown using Equation 11.15 and Equation 11.16 that the thermoelectric figure-of-merit for the ring-structure thermocouple is the same as that of the plate-like structure. Since the conversion efficiency of a thermoelectric generator is dependent on temperatures and the figure-of-merit only, the expression for conventional modules (e.g., Equation 11.4) also applies to the ring structure. However, since the

maximum power output is dependent on the thermocouple geometry, it will be different and is given by

$$P_{\max} = \frac{N\pi t(\alpha_n - \alpha_p)^2 \Delta T^2}{2(\rho_n + \rho_p)\ln(r_o/r_i)} = \frac{N\pi t\alpha^2 \Delta T^2}{\rho \ln(r_o/r_i)} \quad (11.17)$$

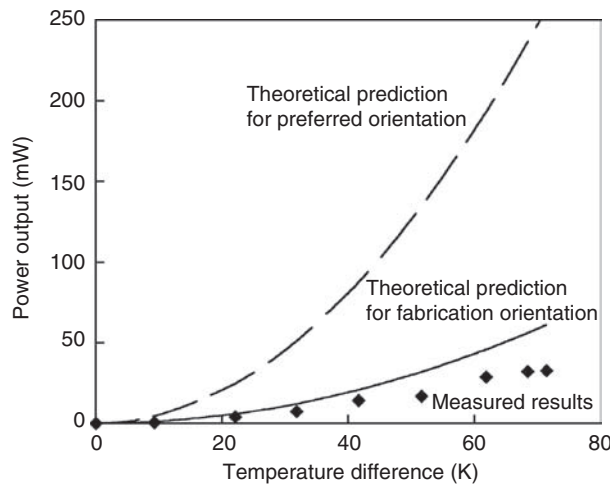
where  $N$  is the number of thermocouples in a converter. An experimental investigation of the ring-structured thermoelectric converter has been carried out based on a basic unit fabricated from four thermoelement rings of  $\text{Bi}_2\text{Te}_3$  based alloys. The ring is 2 mm thick with outer and inner diameters of 14 and 6.4 mm, respectively.

Figure 11.15 shows the power output as a function of temperature difference for the reported ring-structure thermoelectric converter. The rings were not fabricated in the preferred direction of  $\text{Bi}_2\text{Te}_3$  alloys due to difficulty in fabrication processes. Experimental results are represented by diamond-shaped dots and theoretical prediction from Equation 11.17 is represented by the solid line. It can be seen that the theory agrees approximately with the experiment. Errors may be due to inaccurate measurement of temperature difference across the tube, very small internal resistance ( $\sim 7 \text{ m}\Omega$ ) of the thermoelectric converter, and neglecting the thermal and electrical contact effects in the model.<sup>15</sup> The dashed line in Figure 11.15 shows the theoretical prediction of the power output obtained from the similar ring structure module but fabricated in the preferred orientation. Substantial improvement is achievable.

The ring structure provides an ideal configuration for symbiotic applications where heat and power cogeneration are required or advantageous.<sup>8</sup> For example, a thermoelectric converter can be employed to transport hot fluids and generate electrical power simultaneously. Potential applications include undersea oil pipelines, cooling pipes for power station transformers, and domestic hot water pipelines for bath, shower, kitchen, and central-heating systems. It can also be used in a regenerative thermoelectric combustion system for heat recirculation and generating electrical power.<sup>16,17</sup>

The ring-structure thermoelectric converter can also be employed for cooling applications. It is particularly advantageous when heat pumping is in a radial direction. Similarly, the figure-of-merit and the COP of a ring-structure thermoelectric converter will be the same as that of conventional plate-like converters. However, the maximum heat pumping capacity is different and can be expressed as

$$Q_{\max} = \frac{N(\alpha_n - \alpha_p)^2 T_c^2}{2R} = \frac{N\pi t\alpha^2 T_c^2}{\rho \ln(r_o/r_i)} \quad (11.18)$$



**FIGURE 11.15** The power output as a function of temperature difference for the ring-structured thermoelectric converter.

A further advantage of the ring-structure thermoelectric converter is that heat transport occurs in a radial direction. This encourages heat conducting from inside to outside while discouraging the opposite. It has been reported that the thermoelectric performances can be increased by employing tipped thermoelements.<sup>17</sup> The ring-structure is essentially a two-dimensional tipped configuration and consequently some improvements in thermoelectric performances are anticipated.

## 11.8 Summary

The design theory described in this chapter was developed to improve the accuracy of the modeling of thermoelectric modules. It provides useful procedures and guidelines for module optimization based on the economic factor and for obtaining further improvement in the module's thermoelectric performances. The module design is a compromise between the requirements for maximum power output and those for maximum conversion efficiency (in the case of power generation), or between maximum heat pumping capacity and maximum COP (in the case of refrigeration). The introduction of the  $F$  factor provides manufacturers with a useful measure of the quality of module fabrication processes. The theory also provides important insight into understanding the problems encountered in the design and fabrication of micro/nano thermoelectric converters. A model for horizontal structure thermoelectric microcoolers has been developed. Theoretical analysis based on this model indicates that a practically useful cooling effect may be obtained employing standard IC technology. To obtain further improvement, a major challenge is to improve the thermal and electrical contact properties. The ring-structure configuration provides many advantages over the plate-like configurations when heat transport is in a radial directions. The theory for the ring-structure modules has been developed and the results of an analysis based on this theory indicate that the  $ZT$  value, conversion efficiency, or COP of ring-structure module remains approximately the same as that of plate-like configurations. However, the power output or heat pumping capacity of ring-structure modules differs from that of plate-like modules. A preliminary investigation showed that the theory is in good agreement with the experimental data. It is to be noted that the theory for ring-structure modules was derived without taking into account thermal and electrical contact resistances. Consequently, it can only be valid for the cases when the difference between the outer and inner diameters is relatively large.

## References

1. Ioffe, A.F., *Semiconductor Thermoelements and Thermoelectric Cooling*. Infosearch, London, 1957.
2. Min, Gao and Rowe, D.M., Optimization of thermoelectric module geometry for waste heat electric power generation, *J. Power Sources*, 38, 253–259, 1992.
3. Min, Gao and Rowe, D.M., Modified model for calculating the power output of thermoelectric generator, pp. 130–133. *Proceedings of 1st Young Scientists Conference*, Yunnan Province, P R China, 1992.
4. Min, Gao and Rowe, D.M., Peltier device as a generator. In *CRC Handbook of Thermoelectric*, D.M. Rowe, ed., pp. 479–488. CRC Press, New York, 1995.
5. Rowe, D.M., Min, Gao, and Williams, S.G.K., Improving the power output and conversion efficiency of Peltier modules when used as generators, pp. 291–294. *Proceedings of 14th International Conference on Thermoelectrics*, St. Petersburg, Russia, 1995.
6. Rowe, D.M. and Min, Gao, Design theory of thermoelectric modules for electrical power generation, *IEE Proc.-Sci. Meas. Technol.*, 143(6), 351–356, 1996.
7. Rowe, D.M. and Min, Gao, Evaluation of thermoelectric modules for power generation, *J. Power Sources*, 73, 193–198, 1998.
8. Min, Gao and Rowe, D.M., Symbiotic application of thermoelectric conversion for fluid preheating/power generation, *Energy Convers. Manage.*, 43, 221–228, 2002.

9. Min, Gao, Rowe, D.M., Assis, O., and Williams, S.G.K., Determining the electrical and thermal contact resistances of a thermoelectric module, pp. 210–212. *Proceedings of the 11th International Conference on Thermoelectrics*, Arlington, TX, 1992.
10. Gao Min and Rowe, D.M., Recent concepts in thermoelectric power generation, pp. 365–374. *Proceedings of 14th International Conference on Thermoelectrics*, Long Beach, CA, 2002.
11. Min, Gao, On the feasibility of fabricating thermoelectric microcooler using IC technology, *Chin. J. Refrig.*, 3, 50–55, 1987.
12. Rowe, D.M., Morgan, D.V., and Kelly, J.H., Miniature lower power/high voltage thermoelectric converter, *Electron. Lett.*, 25(2), 166–168, 1991.
13. Min, Gao, Rowe, D.M., and Volklein, F., Integrated thin film thermoelectric cooler, *Electron. Lett.*, 34(2), 222–223, 1998.
14. Min, Gao and Rowe, D.M., Cooling performance of integrated thermoelectric microcooler, *Solid-State Electron.*, 43, 923–929, 1999.
15. Min, Gao and Rowe, D.M., A novel ring structure thermoelectric converter, to be submitted to *J. Phys. D., Appl. Phys.*, 2005.
16. Weinberg, F.J., Rowe, D.M., Min, Gao and Ronney, P.D., On thermoelectric power conversion from heat recirculating combustion systems, pp. 941–947. *Proceedings of the Combustion Institute*, Vol. 29, 2002.
17. Hoyos, G.E., Rao, K.R., and Jerger, D., Numerical analysis of transient behavior of thermoelectric coolers, pp. 76–79. *Proceedings of the 1st International Conference on Thermoelectric Energy Conversion*, Arlington, TX, 1976.